

Varistor development for in-vessel magnetic field coils in nuclear fusion devices

M. Teschke^{1*}, F. Firmbach², T. Hutzler², H.P. Martin², K. Schönfeld², I. Zammuto¹

and the ASDEX Upgrade team

¹Max Plack Institute for Plasma Physics IPP, Boltzmannstr. 2, D-85748 Garching, Germany

²Fraunhofer Institute for Ceramic Technologies and Systems IKTS, Winterbergstrasse 28, D-01277 Dresden, Germany

So called “varistors”, based on doped ceramic materials [6][7][8][9] could provide interesting functionality for future nuclear fusion scientific experiments and power plants. They are of special interest for passive in-vessel coils but also for protection of active in-vessel coil feedthroughs. Due to the special high vacuum, high radiation environment, commercially available components are not sufficient for the required parameters. The IPP¹ decided to start a technology development project in cooperation with the IKTS² to improve parameter space and to demonstrate feasibility of the concepts described in this paper. Also very first results of already developed low-voltage, high current-density varistors are given.

Keywords: varistors, in-vessel coils, passive stabilization loops, overvoltage protection

1 Introduction

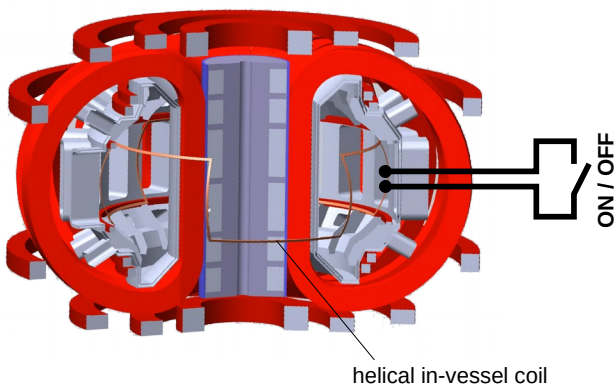


Fig. 1: Helical in-vessel coil for the SPARC experiment [1]. Currently, it is planned to turn on and off this coil by help of an ex-vessel switch.

Upcoming high magnetic field nuclear fusion experiments like SPARC [1], DTT [2] or COMPASS Upgrade [3] are expected to be much more vulnerable for vertical displacement events (VDE), runaway beam (RB) induced damages and loss of first wall tiles due to Halo current forces. Therefore, passive in-vessel coils positioned close to the plasma column were identified to provide improved safety and operation stability by help of counter or dissipative magnetic field generation, see Fig. 1 as an example sketch. The coil energy is directly extracted from the loop voltage of the plasma and transferred to the coil by magnetic induction. Unfortunately, these coils hamper all kind of high-dynamic plasma events, not only the unwanted but also the required ones like plasma breakdown and plasma

current ramp-up. This results in the undesirable situation, that these in-vessel coils need to be switched off during such periods (meaning, the coil conductors must be separated to avoid currents). This dramatically increases technical effort because electric feed-in and out of the expected very high coil currents (several 100 kA...1 MA) for connection to an external high-current switch seem to be almost unfeasible due to extreme Lorentz forces in the high magnetic field environment. An elegant solution would be to introduce active electrical in-vessel components which independently from any control turn-on the coils only in case of plasma loop voltage exceeding a specific voltage threshold (the loop voltage can be directly proportional to the open-loop coil voltage, depending on the coil design). In this case, no external switch and no feed-in and -out of coil currents would be required, at least a huge factor in costs for such coils.

Another challenge is the use of insulating materials in-vessel. Here, it is often observed, that sputtering and radiation modify the surface of materials such that they become more and more conducting over operation time. This can result in a situation where voltage drops become very unbalanced across a toroidal circumference. For example, the insulation of divertor segments is typically realized by help of distance holders based on insulating materials like ceramics, see Fig. 2.

* author's email: teschke@ipp.mpg.de

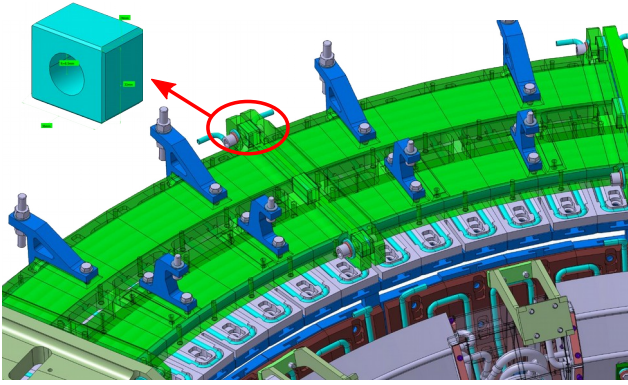


Fig. 2: Electrical insulation of upper divertor modules at ASDEX Upgrade by help of ceramic components [5].

They also take-over mechanical loads (by forming a toroidally stiff ring), thus they are important for mechanical stability of the structure. If some of them get electrically “worse” over time (which means better conducting) their voltage drop is shifted more and more to the less affected (“better”) insulated gaps up to a point where arcing initiates during high dynamic operation phases. This can be easily understood by Fig. 3c. For a constant loop voltage, the voltage drop of low-value resistors (meaning poor isolators) is reduced in contrast to high-value ones (meaning good isolators) due to $V \sim R$. The arcing results in further sputtering and pollution of the plasma which is directly connected to impurity radiation losses. A further consequence can be damaging of the isolators and weakening of the mechanical stability. In present day fusion experiments, this is not a critical issue because the vessel is typically opened and inspected after each campaign. Broken parts can be replaced without high effort. This situation changes dramatically for big experiments after “nuclear phases” with tritium injected, like JET and of course future fusion power plants. Due to high nuclear activation of all in-vessel components, inspection of the vessel interior is only possible by remote handling methods (robots) and very limited, certainly [4].

At the ASDEX Upgrade (AUG) tokamak in Garching/Germany, it was found out early that voltages >100 V per centimeter distance cannot be separated long-term, at least close to the plasma. This is not surprising because even factor thousand smaller electrical field is sufficient for plasma ignition. The plasma current at AUG is ignited at a loop voltage <20 volts for a toroidal circumference of approx. 10 meters. This is equal to an electrical field of 0.2 V/cm [10]. Arcing can be the consequence for comparable higher electrical fields. A good application example where high effort was invested to overcome such technical issues is our “passive stabilizing lopp” (PSL), a special kind of in-vessel coil, see [11], see Fig. 3b. During start of operation of AUG in the 1990th, there were invested many month to find a method to suppress arcing during periods of high loop voltage, e.g. disruptions. The arcing observed

was so intense, that large area of vessel’s first wall became sputtered with copper and radiation losses of plasma too high to continue operation. Finally, high power in-vessel resistors were added in parallel to the “current bridge” (see Fig. 1 in [11]) to convert induced voltage into current – a method good enough to proceed with operation but with the drawback of efficiency reduction of the PSL for large currents (meaning periods of high plasma dynamic where it is most useful). The resistor value was step-wise reduced (during multiple challenging vessel openings) to a value of $125 \mu\Omega$ for an active distance of approx. 1 cm which is a limitation in voltage drop equal to 125 Volts per 1 Megaampere of PSL current. Further investigation of this issue was not performed due to high costs (in operation time of the tokamak). As a consequence, these technical findings were never published.

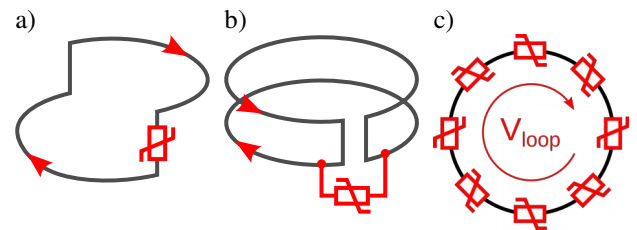


Fig. 3: Three possible applications: (a) activation of in-vessel coils for high induced voltages, (b) arc suppression of components exceeding a specific voltage limit and (c) active balancing of voltages by using varistors as insulators limiting their maximum voltage drop.

For all above mentioned requirements, compare Fig. 3 – (a.) in-vessel switching, (b.) arc suppression and (c.) voltage balancing – it would be helpful to find new engineering solutions. A proposal first time published is presented, here.

2 Varistors

Varistors are non-linear electrical components based on low sintered high-temperature ceramics like doped ZnO [6][7] or SiC [8][9]. The electric behaviour is composed by the serial and parallel inter-connections between the microscopic and manifold (up to 10^6 per mm^3) grains in contrast to e.g. semiconductor Zener diodes which behave very similar but which are typically based on a single (or a very few serial connected), microscopic P/N-doped transition zones. This should be advantageous for applications in nuclear environments with high doses of neutron radiation. Single defects in the ceramic compound should not have a relevant effect on the macroscopic, electric behaviour. Of course, this needs to be proven by future experiments. Anyhow, the IPP integrated a commercial varistor into the ASDEX Upgrade vessel at a plasma exposed position for a full experimental campaign (approx.

7 month of operation). The varistor was not electrically connected, but the breakdown voltage VBD was compared before and after the campaign without identifying any change. Unfortunately, our labs are currently not able to measure a full varistor characteristic as in Fig. 5 for high-voltage (>130V), thus no further details can be given, here.

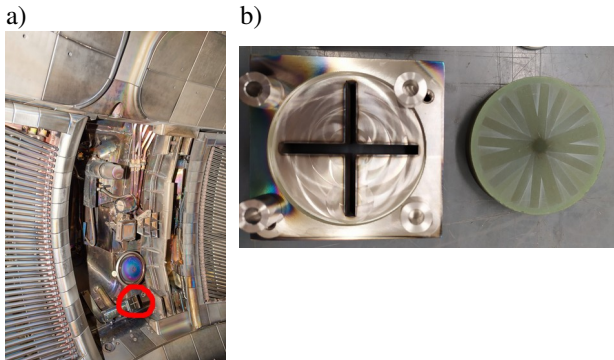


Fig. 4: Commercial varistor integrated into the tokamak vessel of ASDEX Upgrade (a) position at segment 3, (b) removed varistor after a full experimental campaign. The pattern on top of the varistor electrode is even indicating rotation of the disc. This is a strong hint that (parasitic) electrical currents were conducted by the (electrical not connected) varistor leading to Lorentz forces in the high magnetic field environment (up to 3 T).

Another difference to semiconductor based components is the typically much higher energy absorption capability. Commercially available products reach values up to 500 J/cm³ equivalent to approx. 100 kJ/kg. Also the (pulsed) current conduction capability can be high with values above >1 kA/cm² while response speed can be well above >1 kA/cm²/μs.

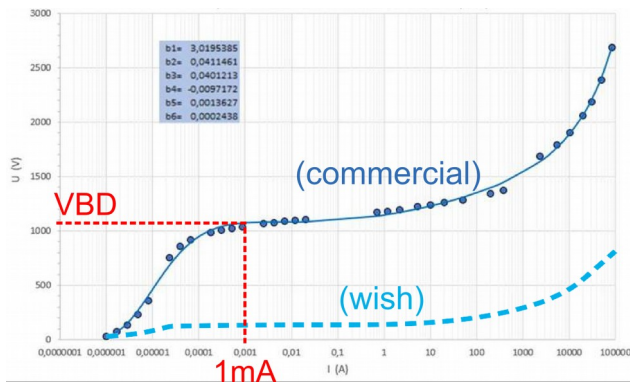


Fig. 5: Typical V/I characteristic of a commercial available varistor disc of 1 cm thickness (dark blue curve, VARS company). The VBD value is often taken at a current of 1 mA. Note the x-axis in logarithmic scale. The light blue curve is discussed in chapter 3.

As already mentioned, the electric characteristic is very similar to a Zener diode (in reverse direction) and an example is shown in Fig. 5. Up to the VBD (or breakdown electric field EBD as material parameter independent from component dimensions) the material behaves like a passive insulator conducting no relevant currents while separating a voltage between its two ends. Exceeding VBD, the weakest contact zones between grains in the material start to conduct. This locally minimizes the electric field but it increases for the other contact zones. An avalanche is initiated ending in a fully conducting body of the varistor ceramic (while overtaking a voltage drop at the same time). Due to the very fast response of the material (kA/μs), eddy currents are induced which superpose with the main current and shift it outwards to the boundaries of the component. This means that power density $J \cdot E$ is not homogeneously distributed over the ceramic body resulting in unbalanced heat loads, different local temperatures and thus thermal stress to the component. This stress can result in cracks and this limit typically defines the max. thermal load accepted by a varistor component. The absolute temperature of the component is typically a much smaller limiting factor because electric behaviour can remain stable up to the sintering temperature which can be well above > 800°C. The acceptable heat load per volume is better for small components for reasons given above (parallel operation of equal units can improve the situation).

Unfortunately, the EBD value of commercially available materials is typically equal or above 1 kV/cm and thus much too high for operation in pre-ionized technical-vacuum environment of a common fusion experiment.

3 Packaging

If a commercial available varistor would be integrated into the vessel, the electric fields at its boundaries would initiate arcing before VBD can be reached. High-vacuum tight packaging would be required to enhance the distance between (outer) electrodes seeing the vacuum environment (and thus reducing the surface electric field), a schema is shown in Fig. 6. Efficient heat removal becomes very challenging while dealing with different thermal expansion rates of the different materials combined, here. Providing mechanical stability and keeping high-vacuum tightness at the same time seems to be extremely hard to realize.

A material with reduced EBD could significantly ease the situation (see “wish” characteristic in Fig. 5). Such varistor can directly be mounted (e.g. soldered) on the massive copper conductors or metallic support structures to provide heat capacity and efficient heat removal without requiring further insulation, see Fig. 7a. Depending on material properties of these low-voltage varistors, me-

chanical loads can be taken over by additional, parallel mounted standard insulators with better mechanical properties. The overall design remains simple.

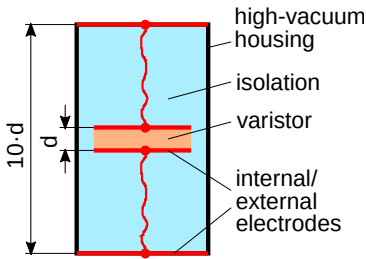


Fig. 6: Packaging of a varistor schema

Another example for a packaging-free application of a low-voltage varistor used to separate different electric potentials of a mechanical structure is shown in Fig. 7b. Here, the varistor is ring-shaped. Without the varistor, the bolt would electrically connect both electrodes but here, the varistor limits the maximum voltage between them, instead. Voltages lower VBD of the varistor disc are accepted and the disc behaves like an isolator. Higher voltages lead to breakdown of the varistor and thus limitation of the voltage.

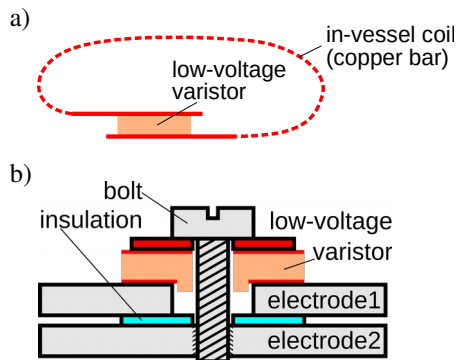


Fig. 7: Two application examples: a) varistor between copper bars of a coil, b) ring-shaped varistor used as voltage limiter (cutaway view). In case of low-voltage varistor, no packaging is required.

4 Material processing

Looking at the situation described above, a specific material development of modified varistor candidates is required. As already mentioned, multiple parameters are of interest additionally to the EBD value like current carrying capability, energy absorption, mechanical properties, but also parasitic body resistivity, nuclear activity and others. Anyhow, the most important parameter to start with is the achievable EBD value. Without finding a material showing $EBD < 0.1 \text{ kV/cm}$, the search for the other properties becomes meaningless related to the planned applications. Thus, for the first feasibility study we focused

exclusively on low EBD values, the non-linearity of the electric characteristic and its thermal stability.

Anyhow, it should also be mentioned, that the importance of current carrying capability differs for the different applications. For voltage balancing, the requirement can be very low, because only small amount of charge has to be balanced in dominant electrostatic (capacitive) arrangements. For high current switching of in-vessel coils or arc suppression, the demand for a high-current capability is obviously much more essential.

IKTS² started with a computer based literature research ([SciFinder](#)) to identify potential materials with $EBD < 0.1 \text{ kV/cm}$. The ceramics based on TiO_2 , WO_3 , ZnO , SnO_2 and SnO_2 / Zn -spinel were considered as promising varistor types with concern to previous experiences. The outcome of the research tool delivered hundreds of publications regarding the above ceramics in combination with varistor effect. A more detailed study was performed for about 20 papers which were regarded as most relevant for the defined objective.

ZnO [12][13][14] and SnO_2 [15][16][17] are already well established ceramics in the field of varistors. Their EBD parameter can be modified by the structure and doping. But the reached level of EBD is higher than required in most papers. A closer EBD could be reached by WO_3 ceramics which can be doped by La, Er Nd and other or can be even used without any doping achieving EBD in the level of 40 V/cm [18]. The most promising ceramics by literature are TiO_2 and SnO_2/Zn -spinel which reach EBD of 33 [19] or 88 [20] V/cm as doped TiO_2 ceramic. The SnO_2/Zn spinel ceramics are reported with EBD of 59 [21] and 87 [22] V/cm . These ceramics are doped as well by Si and Mn.

The EBD range is determined by the sintering parameters, additionally. Sintering temperatures, dwell time and atmosphere in combination with the composition of the ceramic produce specific microstructure and crystalline phases and grain boundaries. This obtained structure defines the resulting EBD basically. Consequently, the EBD can be modified in wide range which needs to be explored thoroughly in advance.

Based on this study, it is clear that the parameter space for interesting materials is enormous. How relevant these materials are for applications needs to be explored.

To gain first experience, 14 different samples were produced: 4x TiO_2 based, 1x WO_3 -based, 3x SnO_2 , 3x ZnO based and 3x Zn_2/SnO_4 -spinel-based.

5 Electrical characterization

For electrical measurement of the (unique and fragile) samples an experimental setup was built to precisely vary voltage while keeping deposited energy under control (and being even able to adjust in a second step). The schematic is shown in Fig. 8.

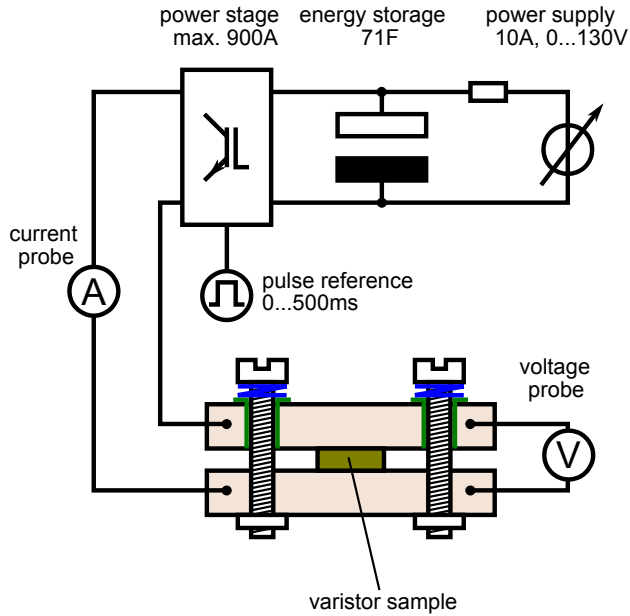


Fig. 8: Experimental setup for measuring the electric characteristic of varistor samples.

It is based on an Ultracapacitor storage, providing the high power necessary for the test but also a duration longer than electrolyte capacitors. Maximum (pulsed) output current capability is well above 1 kA and maximum voltage 130 V. Depending on adjusted voltage, it can deliver up to 600 kJ. The disc-shaped samples having a size of 10 mm in diameter and a thickness in the range of 1-1.25 mm and a weight of approx. 0.3g are expected to accept not more than 0.3 kJ of heat because body temperature would rise above 1000°C. To avoid overheating (and destruction), a programmable and fast IGBT-based powerstage with turn-off capability is interconnected between energy source and load (the sample). The pulse length can be varied between a few μ s and 500ms to limit and adjust the deposited energy independent from the energy storage and voltage level. To provide good electrical contact, the sample (with upper and lower silver electrodes) is pressed between two copper electrodes, which are massive to also provide heat capacity for efficient cooling after the pulse.

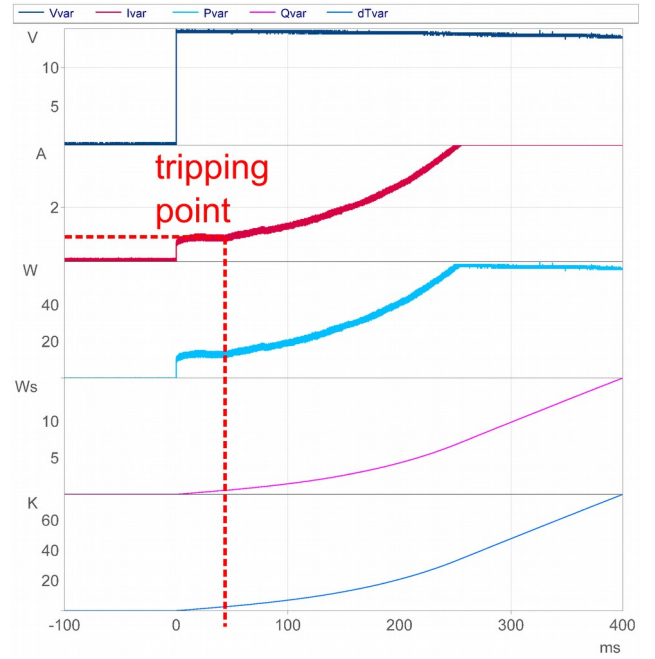


Fig. 9: A measurement of a TiO_2 varistor sample. From upper to lower row, there is shown: the sample voltage, current, power, deposited energy and calculated body temperature rise. Note the 100 ms time scale and the small voltage level.

In Fig. 9 example measurements of the test setup are shown. Note the timescale in the 100 ms range which is very long. The voltage is directly measured at the sample with a separate probe to be current free and to suppress any effect caused by voltage drops between source and load (resistive + inductive drops of wires, powerstage and Ultracapacitor internal resistivity). The current measurement is high-bandwidth (1 MHz) to be sensitive also for short pulses. Deposited heat Q (proportional to energy) is calculated from

$$Q = \int U(t) \cdot i(t) dt$$

The sample temperature on short time scale is estimated by

$$\Delta T = \frac{Q}{C_{p,m} \cdot m}$$

$C_{p,m}$ is the specific heat capacity of the material, e.g. 688 J/(kg·K) for TiO_2 and m the mass of the sample. Cooling can be neglected for short pulses in the millisecond range due to finite heat contact.

From this example it can be seen, that heat influences the electrical properties of the material from a certain tripping point. After this point, the conductivity rises resulting in rising current while the voltage is kept almost constant. This means, deposited power, energy and current density rise rapidly. Destruction of the sample would be the case for long pulses.

In Fig. 10, a collection of measurements for a single sample is shown. For each experiment performed at a different voltage level (achieved by different pre-charging of the Ultracapacitor), a current and voltage sample at a time-point well before the tripping point described above and well after pulse on-set, here at $100\mu\text{s}$, is taken to add it to the V/I -characteristic to be measured. The noisy current signals are filtered and switching events are faded-out before processing the data.

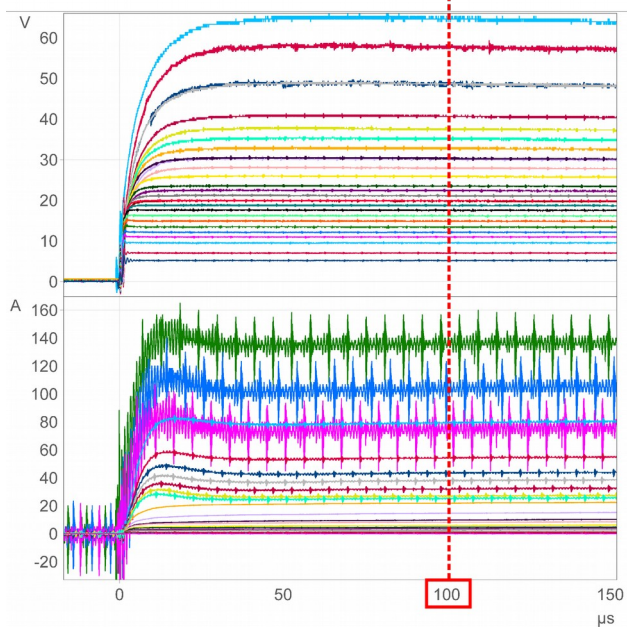


Fig. 10: Multiple measurements at different voltage levels in time. V/I pairs at $100\mu\text{s}$ were taken to identify the electrical characteristic of the samples.

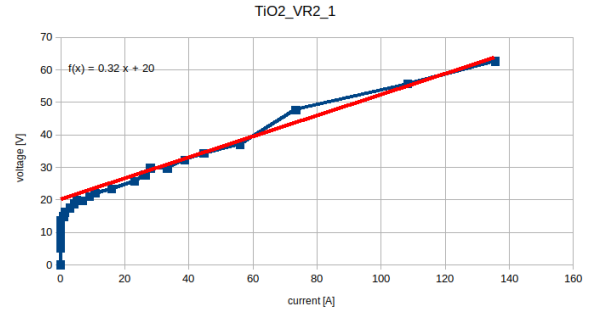
6 Best Results

There were performed multiple high- and low-current measurements for each sample. Many of them are not of interest because they did not show the envisaged varistor behaviour or the parasitic body resistivity was fully covering it (resulting in a linear curve), the material was too brittle to achieve sufficient electric contact or it was damaged after the first measurement.

Therefore, we focus on the most promising results, which were achieved for a TiO_2 and a Zn_2SnO_4 sample with $\text{VBD} < 28\text{V}$, equal to $\text{EBD} < 0.25\text{kV/cm}$, see Fig. 11. The direct comparison to the commercial example in Fig. 5 is possible by taking the geometry into account: The voltage must be multiplied by the thickness ratio: $h_{\text{VARSI}}/h_{\text{IKTS}} = 10/1.25 = 8$ and the current by the area ratio: $A_{\text{VARSI}}/A_{\text{IKTS}} = 80^2/10^2 = 64$. The energy absorbance was possible up to 60J which is equal to 200kJ/kg . The highest current density measured was approx. 0.2kA/cm^2 . The non-linearity is much better for the TiO_2 sample and the high current resistant was measured to be constant at

0.32Ω for a wide range of current, which is equal to a conductivity of 40S/m . This is probably not sufficient for ambitious high current applications like switching coils (Fig. 3a), but definitely good enough for voltage balancing (Fig. 3c) and some arc suppression applications.

a)



b)

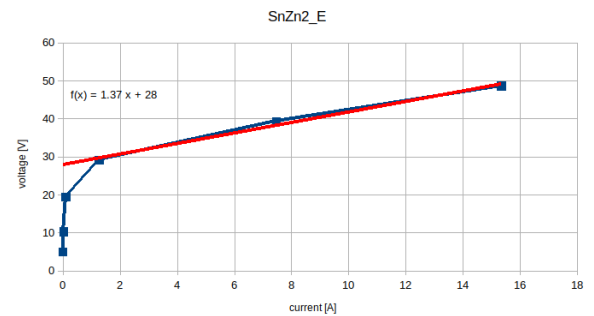


Fig. 11: V/I characteristics of the most promising samples, an (a) TiO_2 and a (b) Zn_2SnO_4 -based varistor disc.

7 Summary and Conclusion

The development of materials showing a varistor effect at small voltage per material thickness could be advantageous for integration of in-vessel coils into fusion devices and other applications from engineering point of view. In the frame of a feasibility study, the production of small samples made of carefully chosen, different ceramic composites was initiated. The electrical characteristic of these samples was measured for a wide current and voltage range. It could be shown that the EBD value was reduced by a factor 4 in comparison to commercially available materials, while even factor 2 higher values in energy deposition before destruction (probably due to small sample size). Also achieved maximum current carrying capability and non-linearity in V/I -characteristic were promising for the best samples. A sample of the same size as the varistor in Fig. 5 would have reached the 10kA high current region.

It has to be pointed out that the results given here were achieved without any optimization cycle in material processing. The development of such materials has just be-

gun. Further steps and experiments are needed to optimize and qualify for fusion applications.

8 Acknowledgements

Special thanks to Antonio Magnanimo for support with the experimental setup.

This work has been carried out within the framework of the EUROfusion Consortium, funded by the European Union via the Euratom Research and Training Programme (Grant Agreement No 101052200 — EUROfusion). Views and opinions expressed are however those of the author(s) only and do not necessarily reflect those of the European Union or the European Commission. Neither the European Union nor the European Commission can be held responsible for them.

References

- [1] Tinguely R.A. et al, 2021 Nucl. Fusion 61, 124003, <https://doi.org/10.1088/1741-4326/ac31d7>
- [2] Belardi V.G. et al, 2021 Mat.Sci.Eng. 1038, 012075, <https://doi.org/10.1088/1757-899X/1038/1/012075>
- [3] Patel N. et al, 2021 Fus. Eng. Des. 171, 112568, <https://doi.org/10.1016/j.fusengdes.2021.112568>
- [4] Tesini A. et al, 2008 Fus.Eng.Des. 83, pp. 810-816, <https://doi.org/10.1016/j.fusengdes.2008.08.011>
- [5] Herrmann A. et al, 2019 Fus.Eng.Des. 146, <https://doi.org/10.1016/j.fusengdes.2019.01.114>
- [6] Clarke D.R., 1999 Am. Cer. Soc. 82(3), <https://doi.org/10.1111/j.1151-2916.1999.tb01793.x>
- [7] Gupta T.K., 1990 Am. Cer. Soc. 73(7), <https://doi.org/10.1111/j.1151-2916.1990.tb05232.x>
- [8] Garcia L.F. et al, 2022 Europ.Ceram.Soc 42, pp. 600-607, <https://doi.org/10.1016/j.jeurceramsoc.2021.10.034>
- [9] Modine F.A. et al, 1988 Appl. Phys. 64, pp. 4229-4232, <https://doi.org/10.1063/1.341289>
- [10] Gribov Y. et al, 2007 Nucl. Fusion 47, pp. 385-403, <https://doi.org/10.1088/0029-5515/47/6/S08>
- [11] Vorpahl C. et al, 2013 Fus. Eng. Des. 88, pp. 537-540, <https://doi.org/10.1016/j.fusengdes.2012.12.028>
- [12] Ismail N.Q.A. et al, 2020 Asian Cer. Soc.8(3), pp.909-914, <https://doi.org/10.1080/21870764.2020.1793472>
- [13] Feng H. et al, 2010 Alloys Comp. 497, pp. 304-307, <https://doi.org/10.1016/j.jallcom.2010.03.047>
- [14] Aldo B., Vernon L., 1991 App.Phys. 70(11), pp. 6883-6890, <https://doi.org/10.1063/1.349812>
- [15] Zang G.Z., Chu R.Q., Xu Z.J., 2020 Bull. Mater. Sci. 43, <https://doi.org/10.1007/s12034-020-2039-2>
- [16] Tominc S. et al, 2020 Eur.Cer.Soc. 40 5518-5522, <https://doi.org/10.1016/j.jeurceramsoc.2020.03.062>
- [17] J.A. Aguilar-Martinez, M.M. Henandez, A.B. Glot, G. Ramirez-Lucero, M.I. Pech-Canul; Effect of Sb2O5 doping and sintering temp-on varistor properties of SnO2-Co3O4-based ceramics; Congreso Internacional de Metalurgia y Materials Articulo 15 (2006) <https://cimav.repositorioinstitucional.mx/jspui/bitstream/1004/1544/1/2006-2.pdf>
- [18] Zhao Hongwang et al, 2010 Jour. Semicon. 31(2) 023001, <https://doi.org/10.1088/1674-4926/31/2/023001>
- [19] Peng F., Zhu D., 2018 Cer. Int. 44 21034-21039, <https://doi.org/10.1016/j.ceramint.2018.08.139>
- [20] Li C. et al, 2001 Mat.Sc.Eng. 85, pp. 6-10, [https://doi.org/10.1016/S0921-5107\(01\)00563-3](https://doi.org/10.1016/S0921-5107(01)00563-3)
- [21] Guo-Zhong Zang et al, 2016 Cer.Int. 42(16), pp. 18124-18127, <https://doi.org/10.1016/j.ceramint.2016.08.125>
- [22] Guo-Zhong Zang et al, 2019 Mat.Sci.:Mat.Elec. 30(4), <https://doi.org/10.1007/s10854-019-00670-0>